

ENCIT-2018-15949

EXPERIMENTAL STUDY OF BOILING PHENOMENON IN THE EVAPORATOR OF A GLASS THERMOSYPHON

Diógenes O. Souza
Ramaiana M. Davies
Cesar A. Barddal
Paulo H. D. Santos
Eduardo N. Santos
Marco J. Silva
Sarah N. Argentin

Multiphase Flow Center (NUEM), Federal University of Technology - Paraná (UTFPR), Av. Sete de Setembro, 3165 - Rebouças
CEP 80230-901 - Curitiba - PR - Brasil
dio_ol@yahoo.com.br
ramaiana@alunos.utfpr.edu.br
psantos@utfpr.edu.br
cesar_barddal@hotmail.com
e.n.santos@ieee.org
mdasilva@utfpr.edu.br
sarahargentin@alunos.utfpr.edu.br

Thiago A. Alves

Federal University of Thecnology – Paraná (UTFPR), Rua Monteiro Lobato, s/n – Jardim Carvalho CEP 84016-210- Ponta Grossa - PR – Brasil
thigoalves@utfpr.edu.br

***Abstract.** Solar collectors assisted by thermosyphons has become an alternative for water heating for home environments due to its clean source of energy. However, for the correct development of the thermosyphons specific correlations are necessary for the boiling and condensation processes which occur within them. There are several studies regarding on correlations for the boiling process in thermosyphons and each one has a different focus: some correlations analyze the pool boiling process, others one film boiling and there are still those that analyze both processes by varying the filling charge ratio. In this work, the pool and film boiling processes and the transition between each boiling regimes are experimentally analyzed for a thermosyphon with filling charge ratio of 100% (in relation to the evaporator volume). An experimental set up was constructed with a glass thermosyphon for testing using water. It was used advanced technology of measurement regarding on two-phase flow and for that two wire-mesh sensors were installed to measure flow hydrodynamic parameters (void fraction, bubble velocity, piston length, frequency of bubbles passage). The heat transfer rate will be varied from 60 to 100 W in steps of 10 W. The values obtained will be analyzed according to the predictions of the theory of boiling, based on several bibliographies*

Keywords: Thermosyphons, Evaporator, Boiling regimes, Wire-mesh sensor

1. INTRODUCTION

The use of solar energy has become popular since recent years as an alternative source of clean energy, especially in home environments. Solar collectors assisted by thermosyphons can increase the transfer of heat to the water that must be heated. Thus, for the development of this type of solar collectors, it is necessary the coefficient of heat transfer related to the flow of the phase-changing fluid inside the thermosyphon.

At boiling high heat transfer rates can be obtained with small variations in temperature (phase change). The high coefficients of heat transfer associated with boiling make its application attractive to several engineering applications (Incropera, et al., 2007) in this study will be analyzed a solar collectors assisted by thermosyphons.

A thermosyphon is an enclosed vertical tube characterized by an evaporator, an adiabatic region and a condenser. The phase change phenomena that occur within the evaporator and condenser sections are boiling and condensation, respectively. These phenomena were studied and, as a result, the two-phase heat transfer correlations were obtained for pool boiling (Cooper, 1984) and for film boiling in vertical and horizontal tubes (Kandlikar, 1990); (Khodabandeh, et al., 2002) and (Khodabandeh, 2005). However, these correlations do not take into account experimental data such as void fraction and filling charge ratio.

Noie (2005) analyzed a closed copper thermosyphon and the influence of the fill ratio and the aspect ratio in determining the boiling heat transfer coefficient in the evaporator. Imura and Sasaguci (1984) studied the critical heat flux and compared the experimental data with the various existing correlations. Boiling and transition regimes were studied for a closed thermosyphon (Niro and Beretta, 1990) and they determined limits regarding on the boiling regimes as a function of the heat flux.

It was observed that in all these experimental studies, the methodology is very similar for the estimation of the boiling heat transfer coefficients. Thus, the coefficient is estimated indirectly using temperature and heat transfer rate. To the best of authors knowledge, there is no application of wire-mesh sensors in order to measure the void fraction and others hydrodynamics parameters for estimation of boiling heat transfer coefficients.

2. EXPERIMENTAL SET-UP

An experimental set-up was constructed at NUEM/UTFPR facilities to study the phenomena of boiling heat transfer in the thermosyphon evaporator. The thermosyphon was developed using a glass tube with internal diameter of 25.6 mm and external diameter of 30 mm with 875 mm of length. The methodology for the development, testing and analysis of thermosyphon was based on (Peterson, 1994) and (Reay and Kew, 2006). The filling charge ratio, which is the ratio of the volume occupied by the working fluid to the total volume of the evaporator, was set at 100%. The thermosyphon has an evaporator length of 320 mm, a condenser of 475 mm and there is no adiabatic region. The evaporator region was heated using an electrical resistor (copper-zinc metal alloy). The ribbon metal alloy was directly connected with a power supply (Agilent U8002A) to provide the heat loads. The evaporator was insulated in order to guarantee that most heat was transferred to the working fluid inside the thermosyphon, minimizing heat leaks to ambient.

Temperatures along the thermosyphon were measured using thermocouples (Type T and J), fixed at outer surface of the evaporator, insulation and condenser. Two thermoresistors (RTD Pt100) were used to measure the internal temperature of the vapor flow and two pressure transducers (Omega PX419, absolute pressure up to 3.45 bar) were used to measure the internal pressure at two points inside the evaporator. Temperatures and pressure were measured using a data acquisition system (Agilent 34970 A data logger) and a computer.

Two wire mesh sensors were installed in the thermosyphon to analyze the flow parameters such as: bubble frequency, bubble length, bubble velocity and void fraction. Such parameters are necessary to delineate the flow patterns that are associated with the boiling regimes and to estimate the boiling heat transfer.

Eight thermocouples were installed at outer surface of evaporator located as shown in Figure 1(a). The photo of experimental apparatus is presented at Figure 1(b).

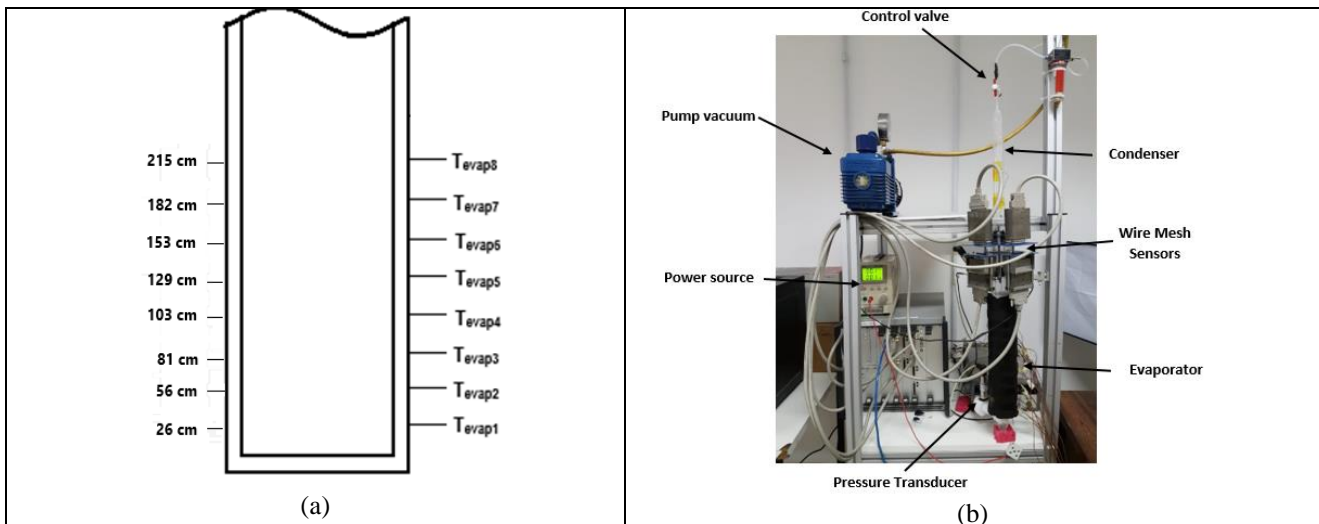


Figure 1. a) Positions of thermocouples in the evaporator. b) Experimental Apparatus.

According to the boiling theory, when the temperature of the inner surface $T_{p,int}$ is higher than the saturation temperature of the liquid T_{sat} corresponding to its pressure, the boiling starts. The heat is transferred from the solid surface to the liquid and the appropriate form of Newton's law of cooling, showing the local heat transfer coefficient, is:

$$h_z^{exp} = \frac{q_{evap}}{(T_{p,int} - T_{sat}) A_{sup,e}} \quad (1)$$

Note that, in Eq. (1), an estimate of temperature of the internal wall of the thermosiphon is required to calculate the convective coefficient inside the thermosiphon. According to Incropera *et al.* (2007), the thermal conduction resistance R can be defined as the ratio between a driving potential and the corresponding heat transfer rate, as shown in Eq. (2).

$$R = \frac{\bar{T}_{p,ext} - \bar{T}_{p,int}}{q_{evap}} \quad (2)$$

where $\bar{T}_{p,ext}$ [°C] is the average temperature in the outer surface and q_{evap} [W] is heat transfer rate dissipated by the resistor by Joule Effect.

For radial systems, as in the case of hollow cylinders, exposed to fluids with different temperatures on the inner and outer surfaces, the thermal resistance has the form:

$$R = \frac{\ln \frac{r_e}{r_i}}{2\pi k_{vidro} L_e} \quad (3)$$

Where r_e and r_i refer to the external and internal radius of the tube wall, k_{vidro} is the thermal conductivity of the thermosiphon material in the case glass and L_e is the length of the evaporator section. Combining the two previous equations, we arrive at the following Eq. (5), an estimate of the average temperature of the internal wall of the thermosiphon:

$$\bar{T}_{p,int} = \bar{T}_{p,ext} - \frac{\ln \frac{r_e}{r_i}}{2\pi k_{vidro} L_e} q_{evap} \quad (4)$$

The gas velocity for an elongated bubble in upward vertical flow can be estimated by conserving the mass for unit cell embedding the bubble and the piston, according to Taitel and Barnea (1990), for steady and unidimensional regime:

$$U_{GB} = U_T - (U_T - U_{GS}) \frac{\alpha_{GS}}{\alpha_{GB}} \quad (5)$$

Where U_{GB} is the gas velocity in the elongated bubble region, U_T is the translational velocity referring to the nose of the bubble; U_{GS} is the gas velocity in the slug region, α_{GB} is the vapor fraction in the elongated bubble region and α_{GS} is the vapor fraction in the slug region. In the case of our thermosiphon we can visually verify that the slug region is composed only of the liquid phase, so we have that $U_{GB} = U_T$. The translational of the elongated bubble and the vapor fraction in the elongate bubble region can be determined by the wire mesh sensor.

Another parameter to be determined is the superficial velocity of the gas (j_g), numerically this velocity is equivalent to the velocity that the vapor phase would have if it were flowing alone and is defined as:

$$j_G = U_{GB} \alpha_{GB} = U_T \alpha_{GB} \quad (6)$$

In order to determine the mass flow (\dot{m}) using the experimental data obtained with the wire mesh sensors, it is necessary to know the velocity of the gas in the elongated bubble region (U_{GB}) which is obtained directly by the sensor, Considering the thickness of liquid film negligible when compared to the diameter of the evaporator and knowing that flow is due to buoyance forces in the gas phase. Actually, the inertia of the elongated bubble pushes the liquid upwards and then the liquid returns by gravity force, flowing towards the film region. Even so, the liquid remains stationary in the average and the liquid superficial velocity can be considered as zero, as a consequence the mass flow rate of the liquid can be neglected. Therefore, the mass flow rate along the evaporator can be approximated to the mass flow rate of the vapor phase:

$$\dot{m} = \dot{m}_G \quad (7)$$

The mass flow rates for vapor phase can be calculated as:

$$\dot{m}_G = \rho_G U_{GB} A_p \alpha_{GB} \quad (8)$$

where A_p [m²] is the inner transversal area of evaporator

The mass flux G [kg/m²s] through a tube of transversal area A [m²] is denoted as:

$$G = \frac{\dot{m}}{A} \quad (9)$$

By means of a balance of energy in the region of the evaporator one can estimate the mass flow \dot{m} [kg/s]:

$$q_{evap} = \dot{m} [c_{pa} (T_{sat} - T_1) + h_{lv}] \quad (10)$$

where c_{pa} [J/kgK] is the specific heat of water, T_{sat} [°C] is the temperature of water in upper end of evaporator and T_1 [°C] is the temperature of water in the bottom end of evaporator.

The resistor is coupled around the evaporator and the power is determined by the voltage V [V] and current i [A] supplied by the power source:

$$q_{evap} = Vi \quad (11)$$

The superficial velocity of the gas can be defined as a function of the quality (X) and specific mass of vapor (ρ_v)

$$j_g = \frac{GX}{\rho_v} \quad (12)$$

Since the mixture velocity J is defined as the sum of the superficial velocities of the phases, then $J = j_g$. Thus, the mixture Reynolds number can be expressed as:

$$Re_m = \frac{\rho_m JD}{\mu_m} \approx \frac{\rho_L U_T R_{GB} D}{\mu_L} \quad (13)$$

where ρ_m [kg/m³] is the specific mass of mixture, μ_m [Pa.s] is the viscosity of mixture, ρ_L [kg/m³] is the specific mass of liquid, μ_L [Pa.s] is the viscosity of the liquid and D [m] is the thermosyphon intern diameter. The mixture properties can be approximated as the liquid ones, since $\rho_L \gg \rho_g$ and $\mu_L \gg \mu_g$ for water at saturated liquid and vapor states on near ambient conditions.

With all the necessary parameters defined, it is possible to estimate the heat transfer coefficient for the boiling regime through the correlation of Kandlikar's (1990):

$$\frac{h_{TP}}{h_{SP}} = 0.6683 \left(\frac{\rho_L}{\rho_G} \right)^{0.1} X^{0.16} (1-X)^{0.64} f_{(Fr)} + 1058 \left(\frac{q''}{G h_{lv}} \right)^{0.7} (1-X)^{0.8} G^* \quad (14)$$

$$\frac{h_{TP}}{h_{SP}} = 1.136 \left(\frac{\rho_L}{\rho_G} \right)^{0.45} X^{0.72} (1-X)^{0.08} f_{(Fr)} + 667.2 \left(\frac{q''}{G h_{lv}} \right)^{0.7} (1-X)^{0.8} G^* \quad (15)$$

where h_{SP} [W/m²K] is the single-phase flow heat transfer coefficient, X is the quality, q'' [W/m²] is the heat flux and h_{lv} is the latent heat of vaporization. The parameter $f_{(Fr)}$ represents the flow stratification for horizontal ducts and can be assumed as unity for vertical flows (Incropera *et al.*, 2007). The parameter G^* depends on the fluid-surface combination and is unity for water-cooper. Here, it is assumed the same value of $G^* = 1$ for water-glass, since this fluid-surface combination was not found in literature. Incropera *et al.* (2007) suggests using the maximum value of h_{TP} between eqs. (12) and (13). The single-phase heat transfer coefficient is estimated by forced convection downstream the vaporization starts using the Gnielinski's (1976) correlation:

$$h_{SP} = \frac{(f_m / 8)(Re_m - 1000)Pr_L k_L}{1 + 12.7(f_m / 8)^{1/2}(Pr_L^{2/3} - 1)} D \quad (16)$$

$$f_m = [0.790 \ln(\text{Re}_m) - 1.64]^{-2} \quad (17)$$

where f_m is the friction factor calculated with the mixture Reynolds number Re_m , Pr_L is the liquid Prandtl number and k_L [W/m.K] is the liquid thermal conductivity. It is important to notice that all the properties mentioned so far are estimated at the saturation temperature T_{sat} in the evaporator

2.1 Wire-Mesh Sensor

The wire-mesh sensor is an intrusive imaging device which provides flow images at high spatial and temporal resolutions and it has been accepted as an alternative technique for multiphase flow tomographic imaging (Prasser, et al., 1998) and (Kesana, et al., 2017). The associated electronics measures the electrical property (e.g. electrical resistance/capacitance) in the gaps of all crossing points which are converted into phase fraction distributions (Da Silva, et al., 2007) and (Dos Santos, et al. 2015). Such sensors have been successfully employed by a number of researchers to investigate different flow phenomena and it is widely used in the generation of numerical modeling of flows (Shaban, et al., 2015) and (Dos Santos, et al., 2017). The sensor comprises of two sets of stainless steel wires stretched over the cross-section with an axial spacing of a few millimeters and an orthogonal angle to each other, thus forming a grid of electrodes. One electrode plane is the transmitter, while the other is the receptor. Further, images generated by the wire-mesh sensor are processed in order to obtain relevant flow parameters (Furuya, et al., 2017) and (Dos Santos, et al., 2016).

In order to obtain the phase fraction distributions, a calibration routine with only and another with is necessary. The resulting 3D matrix of the void fraction $\alpha(i,j,k)$ corresponds to:

$$\alpha(i, j, k) = \frac{V_H(i, j) - V(i, j, k)}{V_H(i, j) - V_L(i, j)} \quad (18)$$

where i and j represents the spatial position of the crossing point and k the temporal index. V_L represents the lower value (air – low permittivity) and V_H stands for higher value (water – high permittivity). To analyze the results void fraction sequences of the flow as well as cross section images from the pipeline can be generate. Integrating this data in space and/or time one can obtain the mean void fraction $\alpha(k)$.

$$\alpha(k) = \sum_i \sum_j a_{i,j} \cdot \alpha(i, j, k) \quad (19)$$

where $a_{i,j}$ is the contribution of each crossing point (i,j) for the total cross section area.

In this work two capacitive wire-mesh sensors 8 x 8 (i.e. 8 transmitter electrodes and 8 receiver electrodes) operating at 2000 frames per second were used in order to determine the phase fraction distribution and phase velocities. Figure 2a depicts the pair of wire-mesh sensor installed at measuring section and figure 2b the electrodes formed by the crossing points of receiver and transmitter wires.

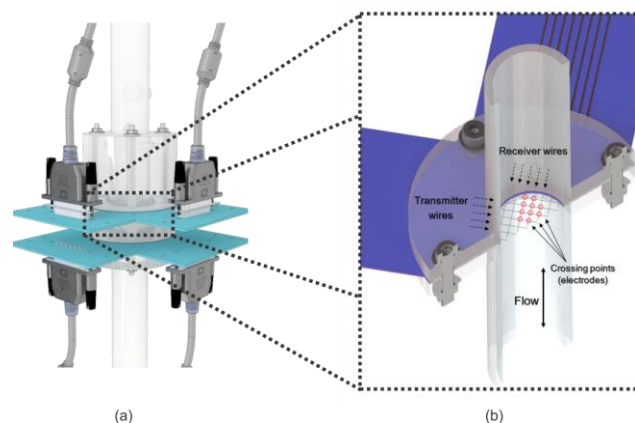


Figure 2. (a) Two wire-mesh sensors installed at measuring test section (b) Transmitter and receiver sets of stainless steel wires stretched over the cross-section.

3. RESULTS

With the aim of analyzing the heat transfer coefficient in the boiling, the first concern is the temperature measurement along the evaporator, so to ensure the accuracy of the data obtained all thermocouples and thermoresistors used in the experimental activity were calibrated.

After the calibration, the thermocouples are properly coupled to the evaporator according to figure 1.a) and through the acquisition system the temperature variation is obtained, figure 3 shows how the temperature variation as a function of time occurs.

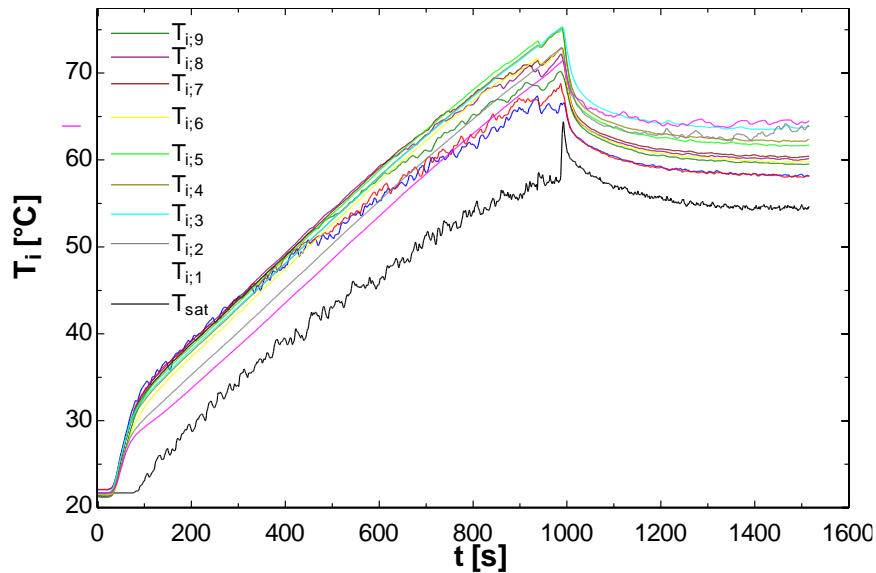


Figure 3. Temperature variation along the evaporator for heat transfer of 70 W

It is observed that after the pump is started, the internal pressure decreases to approximately 50 kPa and consequently the saturation temperature also ($T_{sat} = 55^{\circ}\text{C}$). Note that after 1000 s, the temperatures reach an approximately permanent regime and under these conditions, the beginning of the boiling process was observed.

Figure 4 shows the local heat transfer coefficients during the boiling process for heat loads of 60, 70, 80, 90 and 100 W for filling charge ratio of 100%.

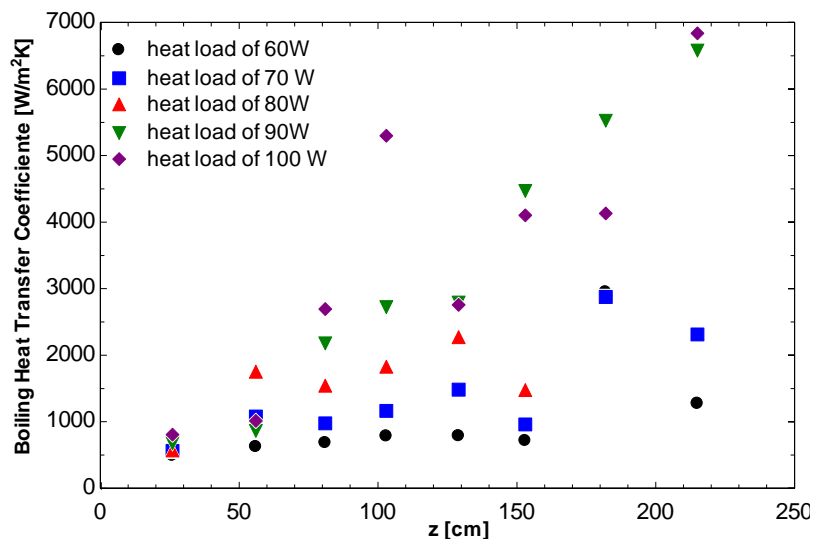


Figure 4. Experimental boiling heat transfer coefficient for several heat loads.

In figure 4 it is shown how the boiling heat transfer coefficient varies in relation to the height of the evaporator and the heat load applied.

The water inside the evaporator is initially subjected to a heat load of 60 W, in this situation, the Boiling heat transfer coefficient values vary from 493 $\text{W/m}^2\text{K}$ corresponding to the lower end of the evaporator (26 cm) to 1277 $\text{W/m}^2\text{K}$ at a height of 215 cm.

For a heat load of 70 W a small increase in the values of the boiling heat transfer coefficient is observed, varying from 562 W/m²K in the position corresponding to thermocouple 1, that is, 26 cm, and a substantial increase in position corresponds to 183 cm, reaching the value of 2876 W/m²K.

When applying a heat loss of 80 W, the average values increase with respect to the heat load of 70 W. The values obtained for boiling heat transfer coefficient vary from 570 W/m²K at the lower end of the evaporator to 2271 W/m²K at the height corresponding to 129 mm. In relation to the measurement obtained in the thermocouples located near the end of the evaporator (thermocouples 7 and 8) some inconsistencies in the measurements, which in the beginning, are due to the condensate return by gravity, which causes the cooling of the intern wall causing the temperature of intern wall is below the saturation temperature.

A considerable increase in boiling heat transfer coefficient values is observed when a heat loss of 90 W is applied. Values range from 676 W/m²K at the lower end of the evaporator to 6577 W/m²K at the height corresponding to 215 mm. For this heat load a certain linearity is observed in the increase of the boiling heat transfer coefficient in relation to the height of the evaporator. This linearity until then had not been observed, but only a tendency in increasing the value. Finally, for a heat load of 100 W, a growth trend of boiling heat transfer coefficient is observed similar to that observed for the heat load of 90 W. The values vary from 920 W/m²K to 6910 W/m²K, respectively in the positions of 26 mm and 215 mm.

The values obtained for the boiling heat transfer coefficient show a tendency for such values to increase with the height of the evaporator and with the heat load applied. An explanation for the values increase with respect to the height of the evaporator is directly linked to the boiling regimes that are observed.

In the first place it should be noted that in regions at the lower end of the evaporator boiling is not observed, in this region the process of heat transfer is due exclusively to natural convection.

When the boiling starts, between the positions related to thermocouples 2, 3 and 4 an increase of the boiling heat transfer coefficient is observed due to the fact that this region is being influenced by the formation of the bubbles causing the beginning of the boiling process.

As the formation of the bubbles intensifies, the formation of larger bubbles that arise due to the coalescence of the smaller ones in this region, related to the thermocouples 5,6,7 and 8, starts to increase in this moment, the values of the boiling heat transfer coefficient increase even more, this fact is explained by the liquid film that is generated due to the formation of the vapor pocket that ignites (slug flow). This liquid film decreases thermal resistance near the region of the inner wall of the evaporator that inhibit the movement of the fluid near the inner surface, and the difference between the internal surface temperature and the saturation temperature decrease, that entails a considerable increase of boiling heat transfer coefficient, thus the formation of the bubbles becomes have a great importance in determining the coefficient of heat transfer. This boiling regime is called boiling in liquid film causing the boiling heat transfer coefficient to increase sharply, as shown in the trend observed in Figure 4.

Finally, it can also be pointed out that the condenser which returns by gravity of the condenser causes the temperature of the inner wall at the evaporator end, in certain situations, to be below the saturation temperature, which does not characterize the phenomenon of pool boiling, in this region the liquid film collapses.

3.1 Wire-Mesh Sensor

Figure 4 shows the void fraction distribution at the measurement test section by flow taking the central vertical wire electrode, i.e. the central chord of the flow.

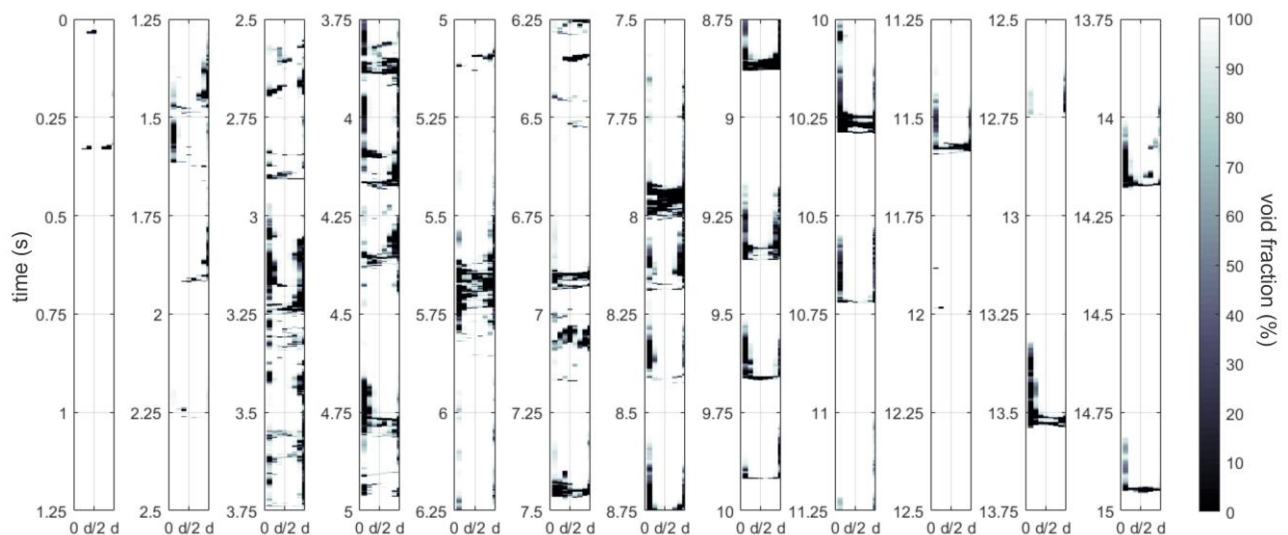


Figure 5. Axial slices images of void fraction distribution

In figure 5 the correspondent time series values for the performed experiment is shown.

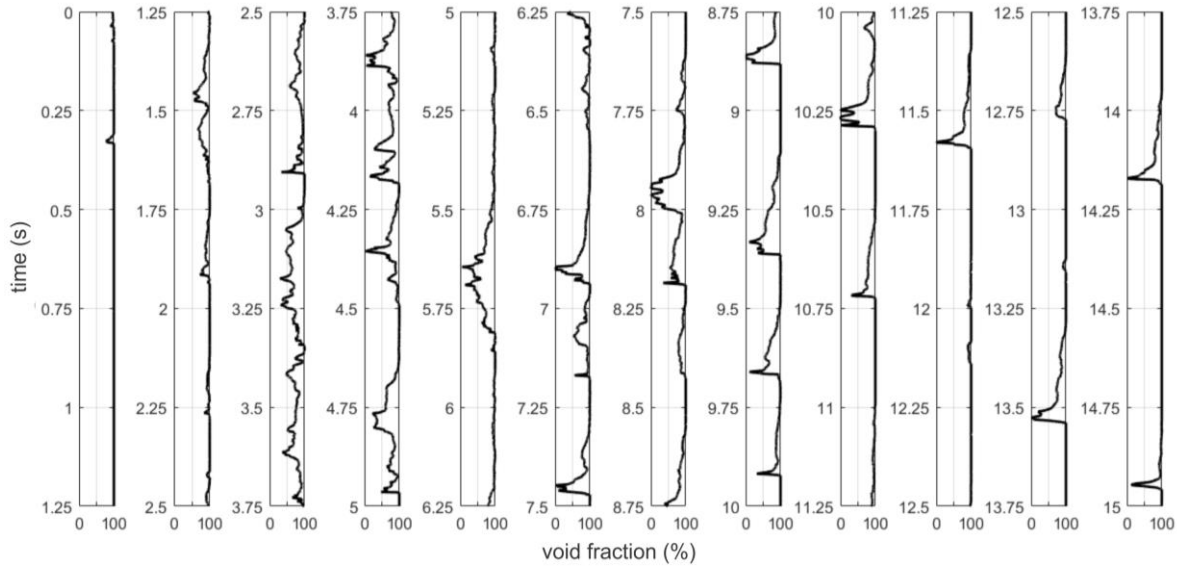


Figure 5. Void fraction time series

These results of void fraction will have used in correlation represented by Eq. (6) for calculation of superficial velocity of bubble where U_{GB} should be determined experimentally through to use of wire mesh sensors. By Eqs. (7), (8), (9) e (10) determined the quality (X). Through the use of Eq. (11) is calculate the Reynolds number of mixture. The heat transfer coefficient for the single phase must be determined through Eqs. (14) and (15). The use of the results obtained in the above equations allows estimation of the boiling heat transfer coefficient through Eqs. (12) and (13) (Kandlikar's correlations) that will be compared with experimental data in order to suggest improvement of correlation results.

Through the use of equations 7 and 8 together with the data obtained with the wire mesh sensor: the mean void fraction, determined through analysed figure 5 and velocity of the vapor phase, the mass flow in the evaporator can be obtained. With the purpose of validating the information regarding the mass flow obtained through the wire mesh sensors, a comparison with the values obtained through the energy balance proposed in equation 10 is performed. The results can be observed in table 1:

Table 1. Mass flow in the evaporator for a heat load of 70 W.

	WIRE MESH	ENERGY BALANCE
\dot{m} [kg/s]	5.21×10^{-4}	5.95×10^{-4}

Table 1 shows that the value obtained with the use of wire mesh sensors, with the reported hypotheses, differed by 14% in relation to the value obtained through the energy balance

4. CONCLUSIONS

The phenomenon of pool boiling in a thermosyphon evaporator was analyzed in this work and some conclusions can be attributed according to the experimental analysis performed. In this article is presented an experimental study of boiling in evaporator of a glass thermosyphon using advanced technology of measurement regarding two-phase flow.

It was verified through the values obtained for boiling heat transfer coefficient that an increase occurs when the heat load supplied to the evaporator is increased. It was also observed that this same coefficient increases as the height of the evaporator increases, this increase is mainly due to the movement of the bubbles near the inner surface of the evaporator, this movement occurs until the coalescence of the bubbles and as the phenomenon occurs it is verified that the boiling heat transfer coefficient values increase substantially.

Another objective is to compare the experimental values obtained for the boiling heat transfer coefficient and the estimated values through the Kandlikar correlation, for this it is necessary to determine mass flow in the evaporator.

Such values are estimated experimentally and through the energy balance providing a percentage error of 14%, an acceptable error within the experimental conditions.

5. REFERENCES

- Cooper, M.G., 1984. "Saturation nucleate pool boiling, a simple correlation". *Int. Chem. Engng. Symp. Ser.*, Vol. 86, p. 785–792.
- Da Silva M. J., Schleicher E. and Hampel U., 2017. "Capacitance wire-mesh sensor for fast measurement of phase fraction distributions", *Measurement Science and Technology*, vol. 18, 2007, pp. 2245-2251.
- Dos Santos E.N., Rodrigues R., Pipa Dr., Morales R.E.M and Da Silva M.J. 2017. "Three-Dimensional Bubble Shape Estimation in Two-phase Gas-liquid Slug Flow", *IEEE Sensors Journal*, vol. 18.
- Dos Santos E.N., Schleicher E., Reinecke S., Hampel U. and Da Silva M.J., 2016. "Quantitative cross-sectional measurement of solid concentration distribution in slurries using a wire-mesh sensor", *Measurement Science & Technology (Print)*, v. 27, p. 015301
- Dos Santos E.N., Morales R.E.M., Hampel U. and Da Silva M.J., 2015. "Dual-modality wire-mesh sensor for the visualization of three-phase flows". *Measurement Science & Technology (Print)*, v. 26, p. 105302
- Furuya M., Kanai T., Arai T., Takiguchi H., Prasser H-M., Hampel U. and Schleicher E., 2017. "Three-dimensional velocity vector determination algorithm for individual bubble identified with Wire-Mesh Sensors". *Nuclear Engineering and Design*.
- Gnielinski, V., 1976. "New equations for heat and mass transfer in turbulent pipe and channel flow". *Int. Chem. Eng.*, Vol. 16, p. 359–368
- Incropera, F. P.; Dewitt, D. P. *Fundamentals of Heat and Mass Transfer*. 6 ed. John Wiley & Sons, Inc., 2007.
- Kandlikar, S.G., 1990. "A general correlation for saturated two-phase flow boiling heat transfer inside horizontal and vertical tubes". *Int. J. Heat Transfer Trans. ASME*, Vol. 112, p. 219–228.
- Kesana N.R., Parsi M., Vieira R.E., Azzopardi B., Schleicher E., McLaury B.S., Shirazi S.A. and Hampel U., 2017. "Visualization of gas-liquid multiphase pseudo-slug flow using Wire-Mesh Sensor", *Journal of Natural Gas Science and Engineering*. Vol, 46, pp. 477-490
- Khodabandeh, R., 2005. "Heat transfer in the evaporator of an advanced two-phase thermosyphon loop". *Int. J. Refrig.*, Vol. 28, p. 190–202.
- Khodabandeh, R., Palm, B., Hagdorn, C., 2002. "Influence of diameter and height of evaporators on the boiling heat transfer in a closed advanced two-phase thermosyphon loop". In *First Scandinavian Conference on Cooling of Electronics*, KTH, Stockholm.
- Imura, H.; Sasaguci, K. and Kozai H., 1983. "Critical heat flux in a closed two-phase thermosyphon". *Int. J. Heat Mass Transfer*, Vol. 26. No.8. pp. 1181-1188.
- Noie, S.H.; 2005. "Heat Transfer Characteristics of two-phase closed thermosyphon". *Applied Thermal Engineering*, Vol 25. p. 496–506.
- Niro, A.; Beretta, G.P.; 1990 "Boiling regimes in a closed two-phase thermosyphon". *Int. J. Heat Mass Transfer*, Vol 33, N° 10. p. 2099-2010.
- Prasser H-M., Böttger A. and Zschau J., 1998. "A new electrode-mesh tomograph for gas-liquid flows", *Flow*
- Shaban H. and Tavoularis S., 2015. "The wire-mesh sensor as a two-phase flow meter", *Measurement Science & Technology* vol. 26, 015306.

6. RESPONSIBILITY NOTICE

The authors are the only responsible for the printed material included in this paper.